COMMISSARIAT A L'ENERGIE ATOMIQUE

CENTRE D'ETUDES NUCLEAIRES DE SACLAY
Service de Documentation
F91191 GIF SUR YVETTE CEDEX

CEA-CONF --10355

L6

SQUIDs. PRINCIPLES AND BASIC APPLICATIONS IN EXPERIMENTAL PHYSICS

OUIO M.
CEA Centre d'Etudes Nucleaires de Saclay, 91 - Gif-sur-Yvette (FR).
Service de Physique des Solides et de Resonance Magnetique

Communication présentée à : Seminar on Low Temperature Experimental Physics

Nara (JP)
9-10 Apr 1990

SQUIDs: PRINCIPLES AND BASIC APPLICATIONS IN EXPERIMENTAL PHYSICS

M. Ocio

Service de Physique des Solides et de Résonance Magnétique

CEN-Saclay, 91191 Gif-sur-Yvette Cedex

I. INTRODUCTION

SQUIDs (Superconducting Quantum Interference Devices) are a new type of devices based on the concepts of fluxoid quantization in a superconductor [1] and Josephson tunnelling [2]. Used as magnetic flux sensors, they can approach sensitivities of order 10^{-19}Wb (10^{-11} gauss/cm^2).

Quantum interference effects between two Josephson junctions in a superconducting loop were observed for the first time in 1964 by Jaklevic et al. [3]. The possible applications for high sensitivity instrumentation were soon realized, and a great variety of d.c. SQUIDs (d.c. means that the device is operated with a direct current bias) were developed with the purpose of studying quantum interference phenomena.

In 1967, first appeared the r.f. SQUID [4] (r.f. since the device is operated with a r.f. flux bias). The r.f. SQUID involves only one Josephson junction in a superconductive loop (it is improperly named since energy absorption by hysteresis takes place, and no interference). Probably because it is easier to develop a device with only one junction, the r.f. SQUID was soon far more widely used than the d.c. SQUID, and several commercial versions were available from the early 1970's.

Only at the beginning of the 1980's, after great improvements in thin film technologies, commercial realizations of d.c. SQUIDs appeared. At the day, elaboration of state of the art devices involves sophisticated photolithographic techniques in the μm range [5,6].

It is not the purpose of the present paper to give a full development of the devices theory since several extensive reviews have been published already [7,8,9]. Instead, the basic principles will be shortly developed, and a part of the paper will be devoted to the description of technical aspects whose knowledge is useful for experimentalists wanting to use SQUIDs.

The last part is devoted to the basic applications of SQUIDs in experimental research, with special emphasis to the low temperature physics experiments.

Seminar on Low Temperature Experimental Physics SPSRM/90-033
April 9-10, 1990, Nara Japan

II. SUPERCONDUCTIVITY

1) Fluxoid Quantization

According to the early London theory [1] (which is sufficient for our purpose here), superconductivity results of the condensation of a macroscopic number of charge carriers into the same quasi-particle quantum state. This condensation was later explained as the consequence of the pairing of some electrons under the action of a virtual phonon exchange mechanism [10]. These pairs (Cooper pairs) are all described by a single macroscopic wave function $\psi_S = \psi_0 \exp(i\varphi)$ whose module is related to the pairs charge density ρ_S : $|\psi_S|^2 = \rho_S$.

Since ψ_S must be single valued, and provided ρ_S is supposed almost constant in the superconductor, integration of the pair generalized momentum around a closed path Γ leads to fluxoid quantization [8]:

$$\mu_0 \lambda^2 \oint_\Gamma \vec{J}_S \mathrm{d}\vec{\ell} + \oint \vec{A}\, \mathrm{d}\vec{\ell} = \frac{\hbar}{2e} \oint_\Gamma \nabla\vec{\varphi}\, \mathrm{d}\vec{\ell} = n\Phi_0 \tag{1}$$

where $\Phi_0 = h/2e \approx 2 \times 10^{-15}$Wb is the flux quantum, λ is the penetration depth ($\lambda^2 = m/(\mu_0 e \rho_S)$) and $\vec{J}_S$ is the pairs current density.

In a ring or cylinder of thickness much larger than λ, one may choose a path far from the edges, where $\vec{J}_S = 0$. Hence

$$\oint_\Gamma \vec{A}\, \mathrm{d}\vec{\ell} = \int_S \vec{B}\, \mathrm{d}\vec{S} = \Phi = n\Phi_0 \tag{2}$$

where $\vec{S}$ is the (oriented) surface supported by Γ.

2) Josephson Tunnelling

Macroscopic quantum tunnelling, between two superconductors weakly coupled by a thin oxyde layer was predicted by Josephson [2]. The wave functions of both sides decay exponentially inside the barrier, leading to a small coupling energy between the two separate Cooper pairs systems. This tends to lock together the phases of the two superconductors. A d.c. supercurrent i_s, function of the phase difference $\Delta\varphi$ can flow, up to a maximum value i_c, the critical current:

$$i_s = i_c \sin \Delta\varphi \tag{3}$$

(The "d.c. Josephson equation").

If a current greater than i_c is passed through the junction, a voltage difference $V(t)$ appears, and the phase difference varies according to the "a.c. Josephson equation"

$$\frac{d(\Delta\varphi(t))}{\mathrm{d}t} = -\frac{2e}{\hbar} V(t) \tag{4}$$

Supercurrent and phase are then related by

$$i_s = i_c \sin\left\{\Delta\varphi(0) - \frac{2e}{\hbar}\int_0^t V(t')\,\mathrm{d}t'\right\} \tag{5}$$

If a constant voltage difference V_0 is maintained across the junction, the supercurrent oscillates at the Josephson frequency

$$\nu = \frac{2e}{h} V_0 = \frac{V_0}{\varphi_0} \tag{6}$$

The analysis outlined above is correct as long as V is smaller than $2\Delta/e$ where Δ is the gap of the supraconductors of the junction. For $V > 2\Delta/e$, normal tunnelling by electrons and hole excitations takes place (Giaever tunnelling [11]). The consequence is that Josephson tunnel junctions exhibit hysteresis as shown in the $i - V$ characteristic displayed in Fig.1a. For SQUID applications, the hysteresis must be removed. This is obtained by shunting the junction with a small resistance R. The $i - V$ characteristic is modified as a function of the relative values of R, L, the stray inductance and C, the capacitance of the junction (typically 2pF for $10 \times 10\ \mu$m). The behavior of the junction is regular if the hysteresis parameter [12]

$$\beta_c = 2\pi \frac{i_c}{\Phi_0} R^2 \left(C + \frac{L}{R^2} \right) \lesssim 1 \tag{7}$$

(see Fig.1b).

The $i - V$ characteristics of shunted Josephson junctions in the non hysteretic regime ($\beta_c \ll 1$) has been extensively analyzed, theoretically [8] as well as by numeric simulations [12]. For $i > i_c$ it is given by

$$V = R \left(i^2 - i_c^2 \right)^{1/2} \tag{8}$$

which corresponds to a dynamic resistance

$$R_D = \frac{\mathrm{d}V}{\mathrm{d}i} = R \left[1 - \left(\frac{i_c}{i} \right)^2 \right]^{-1/2} \tag{9}$$

Tunnel junctions are obtained by evaporation or sputtering techniques, together with thermal oxydation or glow discharge in oxygen. Early tunnel junctions were not stable nor reliable, and other alternative weak links were developed and used in devices. The first is the Dayem microbridge, a narrow constriction linking two evaporated layers of superconductors (see Fig.2b). The second is the point contact bridge which consists of a sharp niobium screw lightly pressed against a niobium block (see Fig.2c). A good review can be found in Ref.[9] and references therein. In the last decade, considerable progress in the μm range thin-film technology resulted in a new generation of very reproducible and reliable tunnel junction devices [5, 6].

III. SQUID DEVICES

1) r.f. SQUID

Historically, the r.f. SQUID was not the first to appear, but it is at the day the most commonly used and commercially available. Its theory has been extensively described [7.13.14] and will be only briefly stated here.

1.a Principles

The r.f. SQUID is a superconducting loop of inductance L (typically $10^{-9}H$) containing a non hysteretic shunted Josephson junction (or weak link) of critical current i_c (Fig.3a).

Fluxoid quantization around a closed path Γ inside the loop reads

$$\oint_{\Gamma} \nabla\varphi \, \mathrm{d}\ell = 2\pi n = \frac{2e}{\hbar} \oint_{\Gamma_1^2} A \, \mathrm{d}\ell + \Delta\varphi \tag{10}$$

The thickness of the junctions can be neglected, so the integral is the total flux across the loop $\phi = \phi_{ext} - L\, i_d$ where ϕ_{ext} is the applied flux $H_\perp S$, and i_d is the circulating current; moreover n can be taken equal to 0 without any loss of generality. Hence,

$$\Delta\varphi + 2\pi\frac{\phi}{\phi_0} = 0 \tag{11}$$

The circulating current is related to $\Delta\varphi$ by the Josephson relation,

$$i_d = -i_c \sin\left(2\pi\frac{\phi}{\phi_0}\right) \tag{12}$$

yielding the relation between the applied and total fluxes

$$\phi = \phi_{ext} - Li_c \sin\left(2\pi\frac{\phi}{\phi_0}\right) \tag{13}$$

which is displayed in Fig.3b for $Li_c/\phi_0 \sim 0.8$. As long as $2\pi\ Li_c/\phi_0 > 1$ the curve of ϕ versus ϕ_0 is multivalued, i.e. hysteresis takes place when the loop is submitted to an alternative external flux. For example, when a periodic flux of amplitude $\lesssim 2\ \phi_0$ with mean value $\phi_0/2$ is applied, the system runs along the hysteresis loop $ABB'A'A$, and absorbs the corresponding energy ΔE ($\Delta E \sim \phi_0 i_c$). On opposite, if the mean flux is 0, with the same amplitude, the representative point remains in the segment DB and no hysteresis takes place. In practical devices, optimal design corresponds to $Li_c \sim \phi_0$.

To be operated, the r.f. SQUID is inductively coupled to a high quality $L-C$ tank circuit (Fig.4a). R_T is the equivalent parallel resistance of the circuit ($R_T = Q\omega L_T$, where ω is the resonant frequency). The tank circuit is excited by a r.f. current i_{rf} at the resonant frequency: a r.f. current $i_T \sim Q\ i_{rf}$ flows in the inductance, and generates a flux $\phi_{rf} = Mi_T$ in the SQUID. A

d.c. current i_{dc} determines the mean flux bias ϕ_{dc} of the SQUID. Hysteresis and energy absorption occur, at values of i_T (and thus of $V_T = L\omega i_T$) depending on the values of i_{rf} and i_{dc}. In that sense, the r.f. SQUID acts as a parametric absorber which governs the quality factor Q of the circuit, and thus the amplitude of the voltage amplitude V_T for a given i_{rf}. For a given value of i_{rf}, the situation is reproduced identically when i_{dc} is shifted by $\Delta i_{dc} = \phi_0/L_T$ (or when ϕ_{dc} is shifted by ϕ_0). The voltage amplitude V_T varies periodically with a period ϕ_0 when i_{dc} (or ϕ_{dc}) is varied for a given value of i_{rf}. The Fig.4b represents these variations for successive optimal values of i_{rf}.

The amplitude of the modulation is proportional to the tuning frequency ω and tank self inductance L_T, and inversely proportional to the coupling constant k between the SQUID and the self inductance [13]; nevertheless k must be such that $k^2 \geq \pi/4Q$ [9].

1.b Operation of the r.f. SQUID

In operation, the SQUID and tank circuit are contained in a liquid ^{4}He dewar, and the tank circuit is coupled to a room temperature r.f. amplifier and detector.

In most of the realizations, the amplifier is a high input impedance system (Q-meter). Coupling is made via a line whose electrical angle is compensated by a capacitance at the input of the amplifier (Fig.5a) [7,13]. This imposes frequencies of about 20-30 MHz maximum, and, in order for the line to be as short as possible, to put the r.f. amplifier at the top of the dewar.

Another way, less used, is to match the tank circuit to 50Ω by means of a line impedance acting as an impedance transformer. For example, in Fig.5b, the impedance of the circuit at the input of the line coil L_L is 50Ω at the working frequency as long as there is no absorption in the SQUID. The mismatch of the circuit varies with the flux state of the SQUID. It is measured by means of a circulator (or directional coupler) followed by a r.f. amplifier (SWR-meter). Any length of 50Ω r.f. cable can be used. Moreover, the system can be operated at frequencies up to 200 MHz [15].

The r.f. voltage modulation amplitude at the level of the tank circuit is rather small (for example, in a current Q-meter design $\partial V_T/\partial \phi_{ext}$ is about 25 $\mu V/\phi_0$ [7]) and r.f. amplifier gains of order 60-80 db are needed. These amplifiers have a high level of $1/f$ noise and poor d.c. stability. To improve the sensitivity, an a.c. modulation at audio frequency smaller than the tank circuit bandwith (typically 100 KHz), is injected in the tank self-inductance, in order to obtain a flux modulation of amplitude about $\phi_0/2$ in the SQUID. The signal at the output of the r.f. detector is lock-in detected at the modulation frequency. At the output of the lock-in, the V/ϕ characteristic is periodic with period ϕ_0 and simply shifted by $\phi_0/4$ as compared to the original one at the output of the r.f. detector (see Fig.6).

On the other hand, the periodic nature of the SQUID response is not very adapted for linear

applications. It is usual to operate it as a null detector in a flux-locked loop made of an integrator and a feedback resistance connected to the tank self-inductance. The stable state of the loop corresponds to

$$\varphi_{ext} - \frac{MV_0}{r_f} = \frac{n\varphi_0}{2} \tag{14}$$

where V_0 is the output voltage of the integrator, M the mutual inductance between the tank coil and the SQUID, and r_f the feedback resistance (see Fig.6). Changes of V_0 are proportional to changes of φ_{ext}, but n can take any integer value (even or odd depending on the polarity of the feedback) and the absolute value of φ_{ext} remains unknown.

The bandwith of the whole system is limited by the modulation frequency f_{mod}. In fact, the time constant of the integrator is chosen as to limit the bandwith at less than $f_{mod}/2$. Then, the frequency response is given by

$$V_0(\omega) = \frac{r_f}{M}\left(\frac{1}{1 + j\frac{r_f}{MG}\omega\,\tau_i}\right)\phi_{ext} \tag{15}$$

where $G = dV_0/d\phi_{ext}$ is the open loop static gain of the SQUID system and τ_i the time constant of the integrator. In practical devices, other time constants are introduced by the amplification chain, filters, etc., and the frequency response is more complicated. But the essential cut-off is due to the integrator, currently around 10-50 KHz.

The time constant τ_i limits the maximum rate of change of V_0. The slew rate of the system (maximum rate of change of φ_{ext} before breaking lock) corresponds to an error flux $\varphi_0/4$ at the input, respective to the lock point: taking $n = 0$ in relation (14) this corresponds to $\phi_{ext} - MV_0/r_f = \varphi_0/4$. If follows that

$$\frac{d\,\phi_{ext}}{dt} = \frac{\phi_0}{4}\frac{MG}{r_f\tau_i} \tag{16a}$$

or

$$\phi(\omega) = \frac{\phi_0}{4}\frac{MG}{r_f\omega\,\tau_i} \tag{16b}$$

where $\phi(\omega)$ is the maximum sinusoidal flux amplitude for linear operation.

To improve the overall stability, sophisticated integrators involving two (or more) poles are currently used in practical SQUID electronics [6]. The analysis of the response in these cases, although mathematically more complicated, is essentially the same.

1.c Noise in the r.f. SQUID

The noise in r.f. SQUID systems originates in the SQUID itself, in the tank circuit, and in the r.f. preamplifier. Both first sources are due to the fluctuations in the flux values at which transition

and absorption occurs in the SQUID loop (see Fig.3) The result is a fluctuation in V_T [16] and an increase of the tank circuit noise [17].

It is usual to express all noise contributions as an equivalent flux noise S_ϕ in the self inductance L of the SQUID, and to derive the energy resolution $S_\phi/2L$. In r.f. SQUIDs the energy resolution can be expressed as

$$\frac{S_\phi}{2L} \sim \frac{1}{\omega}\left[s_{\text{int}}\frac{\varphi_0^2}{L} + s_{\text{tank}}k_BT_e + s_{\text{preamp}}k_BT_N\right] \tag{17}$$

where s_{int}, s_{tank}, s_{preamp} stand for coefficients corresponding respectively to the intrinsic, tank circuit and preamplifier noises [9]; T_e is an effective temperature for the tank and line circuit, and T_N is the noise temperature of the preamplifier. For typical SQUID systems operated at 20-30 MHz, the intrinsic noise is almost negligible and both further contributions are of the same order. Typically, $S_\phi/2L \sim 2\ 10^{-29} J\ \text{Hz}^{-1}$, or the r.m.s. flux noise is $S_\phi^{1/2} \sim 10^{-4}\phi_0\text{Hz}^{-1/2}$.

In current realizations, the SQUID is coupled to external fields by means of a superconducting coil, the input coil L_i (see Fig.6a), whose mutual inductance with the SQUID is $M_i = k\sqrt{LL_i}$ where k is the coupling constant. If S_i is the equivalent current noise power spectrum, the energy resolution at the input is given by,

$$\varepsilon = \frac{L_iS_i}{2} = \frac{S_\phi}{2k^2L} \tag{18}$$

a more realistic parameter than $S_\phi/2L$, because it involves the efficiency of the coupling to external sources.

The energy resolution is inversely proportional to the frequency. Since the voltage at the tank circuit is proportional to the frequency, working at the highest frequencies would result in the highest signal to noise ratio. Unfortunately, this improvement in noise performance is strongly limited since the noise in preamplifiers increases with frequency [18].

1.d Practical realizations of r.f. SQUIDs

A great variety of r.f. SQUID configurations have been used up to now. Earliest versions involved point contact junctions in bulk niobium structures [13]. Then, niobium thin film devices evaporated on quartz tubes, with Dayem microbridges, were widely used. In these times, there were many attempts to obtain low noise by working at high frequencies. A good review of these early studies can be found in Ref.[9].

At the day, several commercial devices are available, and the time of laboratory made systems is completed. One of the first, and a good example, is the toroïdal bulk Nb SQUID by SHE [19]; early devices involved a point contact junction, which was lately replaced by an hybrid design with a Dayem microbridge. The system works at 19 MHz in the Q-meter mode: the energy resolution above 1 Hz is $\varepsilon \sim 10^{-28} J\ \text{Hz}^{-1}$ ($10^{-4}\phi_0\text{Hz}^{-1/2}$), and the slew rate about $3\ 10^5\phi_0 s^{-1}$.

It is essentially the same equation than for a single junction; but here

$$I_c = 2i_c \left| \cos \pi \frac{\varphi_{ext}}{\varphi_0} \right| \tag{29a}$$

$$\Delta\varphi = \Delta\varphi_1(t) + \pi \frac{\varphi_{ext}}{\varphi_0} \tag{29b}$$

Hence, for $I > I_c$,

$$V = \frac{R}{2} \sqrt{I^2 - I_c^2} \tag{25}$$

Fig.7 displays the above behavior. The critical current varies as a function of the flux, by a succession of half cosinusoids of period φ_0. The modulation is complete if $i_{c_1} = i_{c_2}$ (which is never realized in practice). The I-V characteristics is hyperbolic for $\phi = n\ \varphi_0$ and linear for $\phi = \left(n + \frac{1}{2}\right) \varphi_0$. For $I > I_c$ a voltage appears across the junctions; this voltage is modulated with period φ_0.

In real devices, L cannot be neglected. Nevertheless, their behavior is not fundamentally different from the $L = 0$ case. I_c varies periodically as a function of ϕ_{ext} with a period ϕ_0. The amplitude of the modulation decreases for increasing $\beta = LI_{c_{max}}/\phi_0$ (but, always $I_{c_{max}} = i_{c_1} + i_{c_2}$). The relation (25) is no longer valid but it can be considered as a sufficient approximation as long as $I \gtrsim 1.2\ I_c$.

Fig.8 displays the variations of I_c versus ϕ_{ext}, I/V characteristics and V modulation for a device with $\beta = 1$ [9], which corresponds usually to the design of practical devices. An important parameter describing the SQUID efficiency is $(\partial V/\partial\phi_{ext})_I$. It is maximum for $\phi_{ext} \sim \left(n \pm \frac{1}{4}\right) \phi_0$, with a value

$$\left(\frac{\partial V}{\partial \phi_{ext}}\right)_I \sim \pi\ R/4\ L. \tag{26}$$

2.b Operation of the d.c. SQUID

The d.c. SQUID is biased at a nonzero voltage with a d.c. current $I \sim 1.2\ I_c$. Here also, a flux modulation of amplitude $\Delta\phi \sim \phi_0/2$ is applied to the SQUID, and the signal is lock-in detected; moreover, the system is operated also in the flux locked-loop mode. For these purposes, the SQUID equipment involves a small modulation and feedback coil (Fig.10).

For current values of the SQUID parameters, (for example, $L \sim 10^{-9} H$, $I_c \sim 1\ \mu A$ and $R \sim 1\Omega$), the amplitude of the voltage versus flux modulation is of order 1 μV. To amplify such a small signal with a low noise, it is necessary to adapt the SQUID impedance to the input of the room temperature amplifier.

One of the possible ways is to transform the SQUID impedance by means of a resonant tank circuit, tuned at the frequency of the modulation (Fig.10a). This method has been used for 100 KHz

modulation and quality factor $Q \sim 125$ for the tank circuit [21]. At the input of the amplifier, the voltage amplitude is multiplied by Q; the impedance of the circuit at the input of the amplifier is $Q^2 R_D \sim 10^4 \Omega$ (R_D is the dynamic resistance of the junctions given by relation (9)), a good value for FET amplifiers. The main drawback of this method is that the overall frequency response and slew rate of the system are limited by the high Q value of the tank circuit.

Another method is to adapt the SQUID impedance by use of wide-band transformers. An example of realization working at a modulation frequency of 500 KHz is displayed in Fig.10b [6].

In current audio frequency operation, d.c. SQUIDs are used as null detectors in a flux locked-loop whose feedback current is injected in the modulation-feedback coil. The method is exactly similar to what has been described in section III.1.b for the r.f SQUIDs.

2.c Noise in the d.c. SQUID

In d.c. SQUID systems, the main origin of noise is the Josephson noise in the resistive shunts of the junctions [25]. It has been approximately analyzed by Clarke et al. [24] and numerically computed by Tesche et al. [23]. For an optimized SQUID ($\beta \sim 1$) in the ^{4}He temperature range, the voltage noise power spectrum is $S_V(\omega) \sim 16\, k_B T R$. By using relation (26) it corresponds to an energy resolution [26]

$$\frac{S_\phi}{2L} \sim 8\, k_B T\, L/R_D \qquad (27a)$$

or, taking $\beta_c \sim 1$ (relation (7))

$$\frac{S_\phi}{2L} \sim 16\, k_B T (LC)^{1/2} \qquad (27b)$$

Reducing L and C improves the sensitivity of the device but reduces the possibility to couple it to an external field. Moreover the improvement in noise energy obtained by working at low temperature is limited by the preamplifier noise. For $L \sim 10^{-9} H$ and $R_D \sim 1\Omega$, the calculated energy resolution at $4.2K$ is about $10^{-31} J\ \mathrm{Hz}^{-1}$, corresponding to a rms flux noise of $7\ 10^{-6} \phi_0 \mathrm{Hz}^{-1/2}$. These values are somewhat lower than the values obtained in many practical systems [24].

2.d Practical d.c. SQUIDs

The earlier d.c. SQUIDs were point contact devices [27] and the famous SLUG of Clarke [28], made of a blob of soft solder frozen onto a niobium wire. Thin film planar structure with Dayem microbridges were developed further [29,30]. A thin film tunnel junction d.c. SQUID with cylindrical geometry build in 1976 by Clarke and co-workers [24] showed for the first time better sensitivity than the best r.f. SQUIDs of the period. At the day, commercial realizations have sensitivities one order of magnitude better than r.f. SQUIDs. For example, a system proposed by SHE is build around a toroidal hybrid device. The energy sensitivity above 1 Hz is $\varepsilon \sim 10^{-30} J\ \mathrm{Hz}^{-1}$ ($1.5\ 10^{-5} \phi_0 \mathrm{Hz}^{-1/2}$) with a slew rate about $3\ 10^5 \phi_0 s^{-1}$.

At the day, state of the art devices are laboratory prototypes mainly due to the Clarke group (Berkeley USA) and IBM research Center (N.Y. USA). They result from the late progress in μm range thin film technologies. The devices have planar structures with Nb-NbOx-Pb, Nb-NbOx-Nb or Nb-AlOx-Nb tunnel junctions shunted with evaporated layers of Au or Au alloys (AuCu, AuIn). All peripheral coils are directly evaporated on the SQUID chip, which allows to build directly special devices as gradiometers [31]. Energy resolutions of about $\varepsilon \sim 10^{-31} J\ Hz^{-1}$ can be attained with normal electronics [6]. By using a r.f. SQUID as low temperature amplifier, it is possible to decrease the resolution to few $10^{-32} J\ Hz^{-1}$ at 4.2 K (roughly 25 h where h is the Planck constant) [5].

3. Low Frequency Noise and Drift; Summary of Characteristics

At low frequency, below 0.1 – 1 Hz the noise of all SQUID systems becomes $1/f$ like. Apart from the contribution of the electronic parts, the origin of this $1/f$ component is not well established. It can be generated by equilibrium temperature fluctuations in the junctions [32]. Vortex motion in the superconducting shields or in the SQUID itself are also strongly suspected to produce $1/f$ noise. It can have also exotic origins: for example, SHE toroidal SQUIDs are contained in a Cu-Be leak proof tubing, and a brass holder; ^{4}He convection inside the Nb shield develop thermoelectric currents in the metallic parts, which result in an extra amount of low frequency noise [33].

Also, the output of the flux-locked SQUIDs drifts slowly in time. This drift originates (apart from the electronics) in the ^{4}He bath temperature variations: they induces variations of the critical current of the junctions, and also, modifications of the residual trapped fields, through vortex motion in superconductive shields or variation of the susceptibility of metallic parts. Typical values are about $10^{-3}\phi_0$ by day in non-regulated ^{4}He bath [19,20,24].

The principal characteristics of several modern SQUIDs are summarized in Table I. Energy resolution is reported in Fig.11 as a function of frequency.

IV. PRACTICAL USE OF SQUIDs IN LOW TEMPERATURE PHYSICS

Fundamentally, the SQUID is a flux sensitive device. Apart from recent integrated planar gradiometers [31], it is not used currently as a direct sensor. It is usually coupled to a superconductive input coil and can be considered as a perfect zero conductance galvanometer.

The most basic application of the SQUID is the detection of magnetic fields or magnetic field gradients, with an unprecedented sensitivity. It is now widely used in geophysics [34], biology and physiology [35]. In the domain of elementary particles physics, it is involved in magnetic monopole detection [36] and gravitational antennas [26,35].

Basic uses of the SQUID in experimental physics will be described in this section, with special consideration to low temperature physics applications.

1. The Flux Transformer

1.a Measurement of magnetic fields

The SQUID input coil is connected to a superconductive circuit comprising a pick-up coil of self inductance L_e and a twisted pair of stray inductance L_W (Fig.12a). The coil has N turns and surface S, and sees a magnetic field component H parallel to its axis. A variation ΔH induces a flux variation $\Delta\phi_e = NS\Delta H$ in the coil. Flux quantization in the whole circuit (flux transformer) leads to the condition

$$\Delta\phi_e + \Delta i(L_e + L_W + L_i) = 0 \tag{28}$$

where i is the current in the circuit. Then, the flux in the SQUID varies by

$$\Delta\phi_S = M_i\Delta i = \frac{M_i\Delta\phi_e}{L_e + L_W + L_i} \tag{29}$$

$(L_e + L_W + L_i)/M_i = \xi$ is the coupling factor, of current value within the range 200-1000.

Ordinarily, $L_W \ll L_e \sim L_i$: L_e and L_i are currently of order several μH, and L_W represents about 0.3 μH by meter of twisted wire. In (29), we have neglected the coupling between the input coil and the feeback coil, which can be represented by a small modification of the effective M_i value.

With $M_i = k(L_iL)^{1/2}$and neglecting L_W,

$$\Delta\phi_S = S\Delta HN\frac{k(L_iL)^{1/2}}{L_e + L_i} \tag{30}$$

To measure a field, flat coils are useful: then $L_e \propto S^{1/2}N^2$ and $\phi_e = S\Delta HN \propto \Delta HS^{3/4}L_e^{1/2}$. Hence,

$$\Delta\phi_S \propto \Delta HS^{3/4}k\ L^{1/2}\frac{(L_eL_i)^{1/2}}{L_e + L_i} \tag{31}$$

Coupling is optimal for $L_e = L_i$ and S maximum, i.e. $N = 1$ for a given L_e. If the flux noise of the SQUID has a power spectrum S_ϕ, the smallest ΔH which can be detected by $\sqrt{\text{Hz}}$ is

$$\delta H \propto S^{-3/4}\left(\frac{S_\phi}{2k^2L}\right)^{1/2} = S^{-3/4}\varepsilon^{1/2} \tag{32}$$

where ε is the energy resolution of the SQUID (relation (18)).

It must be remembered that the SQUID can be used to measure only *changes* in flux (or fields). It does not provide an accurate way to determine the absolute value of the field, but the highest known sensitivity to field changes, down to $10^{-11} - 10^{-12}$ Gauss $\text{Hz}^{-1/2}$.

The pick-up coil equipment can be adapted to measure spatial derivatives of changes in magnetic fields. As examples, a first order gradiometer coil sensitive to $\partial Hz/\partial z$ is shown in Fig.12.b; Fig.12.c displays a first order gradiometer sensitive to $\partial Hz/\partial x$ and $\partial Hz/\partial y$. All successive degrees N can be build by recurrently adding two $N-1$ structures with opposite polarities (Fig.12.d and e).

Apart from the classical magnetometry uses of the SQUID, in geomagnetism and biomagnetism, a very exotic one was the search for cosmic magnetic monopoles as predicted by Grand Unified Theories [36]. If magnetic monopoles exist in the nature, when one of them crosses a superconductive loop, it must leave in it as an unambiguous signature, a trapped flux $2\phi_0$. That is true watever the loop geometry. After the probably fortuitous, but famous event reported by Cabrera in 1982 [37], a great effort was made to conceive high degree gradiometers, essentially field insensitive, but sensitive to the $2\phi_0$ monopole signature [36]. To state theoretically the possibility for a particle to exist is not enough for it to actually exist: unfortunately, after ten years of continuous hunting, no further event has confirmed the observation of Cabrera.

SQUID magnetometers are used also as displacement detectors, first in gravitational antennas [26], and more recently in a Josephson effect experiment in ^{3}He superfluid [38]. The pick-up coil is a flat spiral parallel to the moving plate which is covered with a superconducting layer. A permanent current is induced in the flux transformer. When the distance between the coil and the plate varies, the flux state of the coil varies and is detected by the SQUID. Sensitivities of about 5 10^{-4}nm can be reached [38].

1.b Measurement of magnetization (Fig.13)

Measurements of samples magnetization is an important application of SQUIDs. The pick-up equipment is an astatic pair (first order gradiometer); the sample is placed inside one of the coils, and it can be moved away during experiment. A magnet surrounding the gradiometer creates a static field H in the experimental space, and the sample adquires a magnetization $m = \chi H$. The astatic pair is insensitive to H, but sees a flux ϕ_e due to the sample magnetization. The difference between the SQUID measures with the sample in and out of the loop is proportional to the static magnetization. The relation between m and ϕ_e is not easy to calculate in general. In the simple case where the sample is a small sphere [14], $\phi_e = 4\pi\ mV/D$ where V is the volume of the sample and D the diameter of the coil. Then,

$$\phi_S = \frac{\phi_e}{\xi} = \frac{4\pi\ mV}{D\xi} \tag{33}$$

Resolutions of about 10^{-8}emu (in magnetic moment) are currently obtained in commercial realizations [22]. Obviously, the SQUID is not here the only cause of noise and great care must be taken to carefully shield external fields and to avoid sample vibrations [9].

1.c Measurement of magnetic thermodynamic fluctuations

SQUIDs have enough sensitivity to permit measurements of equilibrium thermodynamic fluctuations in magnetic materials. The applicability of the fluctuation dissipation theorem (FDT) [39] could be verified this way on disordered-frustrated systems (spin-glasses) [40,41].

Consider a sample of susceptibility $\chi(\omega) = \chi'(\omega) - j\,\chi''(\omega)$ inside a pick-up coil of free self inductance L_0 forming part of a superconductive flux transformer with the input coil L_i (Fig.13.a). The coil impedance becomes $Z = L_0\omega(1 + 4\pi\, q\chi(\omega))$, i.e. the equivalent circuit involves a self inductance $L = L_0\,(1 + 4\pi\, q\chi'(\omega))$ and a resistance $r = 4\pi\, q\, L_0\omega\, \chi''(\omega)$; here, q is a geometrical coupling factor. For current values of χ' ($< 10^{-2}$emu), $L \sim L_0$. Due to the resistive component, a fluctuating e.m.f. is created in the circuit. Its power spectrum is given by the Nyquist theorem and:

$$\overline{i^2}\,(\omega) = \frac{\overline{V^2}_{(\omega)}}{|Z|^2} = \frac{2}{\pi}k_BT\frac{r}{r^2 + (L_0 + L_S)\omega^2} \tag{34}$$

or

$$\overline{i^2}\,(\omega) \simeq 8\,k_BT\frac{\chi''(\omega)}{\omega}\cdot\frac{1}{(L_0 + L_S)^2}\left\{1 - \left(\frac{4\pi\,\chi''(\omega)L_0}{L_0 + L_S}\right)^2\right\} \tag{35}$$

Since $\chi''(\omega) \ll 1$ the term between parenthesis can be neglected and the flux power spectrum in the SQUID is given by

$$\overline{\phi_S^2}\,(\omega) = M_i^2\,\overline{i^2}\,(\omega) \simeq 8\,k_BT\frac{L_0q}{\xi^2}\cdot\frac{\chi''(\omega)}{\omega} \tag{36}$$

where ξ is the coupling factor of the circuit. The same relation can be obtained by considering the power spectrum of the fluctuating magnetic moment. From FDT, [40]

$$\overline{\mathcal{M}^2}\,(\omega) = \frac{2}{\pi}k_BT\frac{\chi''(\omega)}{\omega} \tag{37}$$

The flux power spectrum in the pick-up coil is derived by integrating the effect of a random fluctuation of magnetization (relation (37)) over the whole sample, yielding [42]

$$\overline{\phi_e^2}\,(\omega) = \overline{\mathcal{M}^2}\,(\omega) \times 4\pi\, L_0q = \xi^2\,\overline{\phi_S^2}\,(\omega) \tag{38}$$

In order to reduce the sensitivity of the measuring system to the residual ambient magnetic noise, and to fluctuations of thermal origin through $\partial\chi'/\partial T$, a gradiometer pick-up coil is used [40,41].

Field fluctuations due to eddy currents in conductors can be measured by the same method [40]. At low frequencies, when the skin depth is larger than the transverse dimension of the conductor, the power spectrum is flat, proportional to the conductivity and to the temperature [43]. This is a possible method for low temperature noise thermometry.

2. The SQUID as a Null Detector: bridge configurations

In many laboratory applications, SQUIDs are used as null detectors in bridge configurations. A detailed description and discussion of the performances of these bridges can be found in Ref.[14].

2.a Measurement of magnetic susceptibility

The most commonly used within these bridges is the mutual inductance bridge (Hartshorn bridge), the basic system for susceptibility measurements.

The principle of the bridge is schematized in Fig.15.a. The secondary of the measuring transformer ($L_I - L_p$) is an astatic pair with mutual inductances m_0 and $-m_0$ with the primary. When the sample of susceptibility $\chi(\omega) = \chi'(\omega) - j\,\chi''(\omega)$ is inserted into one of the coils, its mutual inductance becomes $m = m_0(1 + 4\pi\, q\chi(\omega))$. The primary is connected to a source which delivers a voltage $\dot{V} = V_0 e^{j\omega t}$. In the flux transformer, the voltage induced in the secondary is balanced by the transformer $L_1 - L_2$ whose primary receives a voltage $\dot{V}_1$ obtained from $\dot{V}$ by multiplication (factor K) and dephasing (phase φ) : $\dot{V}_1 = K\dot{V}\, e^{j\varphi}$. The balancing transformer has a mutual inductance $M = k_M\sqrt{L_1 L_2}$. At equilibrium, the current i in the flux transformer is zero, or in other words, the sum of the induced e.m.f. is zero. Taking $L_1 = L_2$, the e.m.f. induced $L_1 = L_2$ in the secondary is $\dot{V}_2 = -k_M\dot{V}_1$. Thus:

$$k_M\dot{V}_1 = 4\pi\, q\chi m_0\frac{d\dot{I}}{dt} = 4\pi\, q\chi m_0\frac{\dot{V}}{L_I} \tag{39}$$

where I is the current in the primary of the measuring transformer. Hence:

$$4\pi\, q\chi = \frac{k_M L_I}{m_0}K\, e^{j\varphi} \tag{40}$$

A practical realization due to Giffard et al. [14] is schematized in Fig.15.b.

There are many possible origins for noise, for example the Johnson noise in the primaries L_I and L_1, the Johnson noise due to the resistive component induced by χ'' in the flux transformer (see Sect.IV.1.b). Nevertheless, the most important one is the proper noise of the SQUID, which is equivalent to a fluctuating flux with power spectrum S_ϕ in the flux transformer. At the secondary L_2, it corresponds to a voltage fluctuation

$$\overline{V_2^2} = (L_2\omega)^2\frac{S_\phi}{(L_p + L_i + L_2)^2} \tag{41}$$

or to a fluctuation $\overline{V_1^2}$ related to an error δK

$$\overline{V_2^2} \equiv k_M^2\,\overline{V_1^2} = k_M^2 V_0^2(\delta K)^2 \tag{42}$$

Hence, the sensitivity is given by

$$\delta K = \frac{L_2\omega}{k_M V_0}\cdot\frac{(S_\phi)^{1/2}}{L_p + L_i + L_2} \tag{43}$$

A modified version of the Hartshorn bridge has been used in an automatic feedback system [44] (See Fig.16). Here, the mutual circuit is build directly in the measuring transformer (m_s). A numeric system drives the ratio between the primary ($\dot{I}$) and compensatory ($\dot{i}$) complex currents and the susceptibility is simply proportional to $\dot{i}/\dot{I}$. Despite the noise problem introduced by the heavy digital part in this system, sensitivities of about 2 10^{-9}emu (in magnetic moment) were attained.

2.b Measurement of impedances

The system is rather similar to the mutual inductance bridge (Fig.17.a). Here, the flux transformer contains the unknown impedance Z, and the latter is connected to the voltage source $\dot{V}$ by a known impedance Z_{st}. At equilibrium, $i = 0$ and $\dot{V}_Z = \dot{V}Z/(Z + Z_{st}) = -k_M\dot{V}_1$. It follows after simple calculations that

$$\frac{Z}{Z_{st}} = -\frac{k_M K e^{j\varphi}}{1 + k_M K e^{j\varphi}} \tag{44}$$

A practical realization by Giffard et al. [14] is schematized in Fig.17.b. Noise is due to the SQUID and to the resistive component R of the impedance Z, and can be analyzed as in Sect.IV.2a. Signal to noise ratio about 1.5 $10^{-8}R^{-1/2}$ can be attained.

3. Measurement of Voltage

SQUIDs have been used also in voltmeter configurations. In that case, they loose a great part of their specificity and interest. Nevertheless, such systems have an important application in noise thermometry at ultralow temperatures [14].

Basically, the SQUID is used as a perfect galvanometer in a feedback system absolutely similar to the old galvonometric amplifiers (Fig.18). The voltage source V of resistance R is connected in series with the input coil L_i and a standard resistance R_{st}. A feedback resistor R_f connects the SQUID output to the standard resistor R_{st} (the flux-locked loop of the SQUID is open). At balance, the current i flowing in L_i is zero and the voltage V_{st} across R_{st} balances exactly the source voltage V. Thus, the volmeter has a high input impedance. Discussion of the SQUID voltmeter performances has been given by several authors [14,15]. If $g = V_0/i \gg R_f \gg R_{st}$, and neglecting all spurious inductances in the circuit,

$$\frac{V_0}{V} \simeq \frac{R_f}{R_{st}} \cdot \frac{1}{1 + j\omega\tau_c} \tag{45}$$

where $\tau_c = \frac{L_i}{g} \cdot \frac{R_f}{R}$.

The input impedance is directly derived

$$Z_i = \frac{V}{i} \sim g\frac{R_{st}}{R_f}(1 + j\omega\,\tau_c) \tag{46}$$

The voltmeter noise power referred to the source is given by

$$S_V(\omega) = \frac{S_\phi}{M_i^2}(R + R_{st})^2 (1 + \omega^2 \tau_i^2) \tag{47}$$

where $\tau_i(\omega) = L_i/(R + R_{st})$. Using the energy resolution ε of the SQUID, and since $R \gg R_{st}$,

$$S_V(\omega) \approx 2\varepsilon \frac{R}{\tau_i}(1 + \omega^2 \tau_i^2) \tag{48}$$

One can define a noise temperature by

$$S_V(\omega) = 4\, k_B T_N(\omega) R \tag{49}$$

Hence,

$$T_N(\omega) \approx \varepsilon \cdot \frac{1 + \omega^2 \tau_i^2}{2\, k_B \tau_i} \tag{50}$$

In the low frequency range, the noise temperature is independent of frequency and proportional to the total resistance in the input circuit. In the white noise region, noise temperatures of about $2.5\ 10^{-7} \tau_i^{-1} K$ have been attained with a thin film d.c. SQUID described by Clarke et al. [24]. The qualities of the SQUID voltmeters are interesting for low resistance sources ($< 10\ \Omega$). For high resistances, FET amplifiers cooled at nitrogen temperature can achieve better performances.

ACKNOWLEDGEMENTS

I am grateful to Prof. M. Date, Research Center for Extreme Materials, Osaka University, Japan, and Prof. Y. Miyako, Department of Physics, Hokkaido University, Sapporo, Japan, for their hospitality while part of this paper was written.

REFERENCES

[1] F. London, Phys. Rev. **74**, 562 (1948).

[2] B.D. Josephson, Phys. Lett. **1**, 251 (1962).

[3] R.C. Jaklevic, J. Lambe, A.H. Silver and J.E. Mercereau, Phys. Rev. Lett. **12**, 159 (1964).

[4] A.H. Silver and J.E. Zimmermann, Phys. Rev. **157**, 317 (1967).

[5] M.B. Ketchen and J.M. Jaycox, Appl. Phys. Lett. **40**, 736 (1982).

[6] F. Wellstood, C. Heiden and J. Clarke, Rev. Sci. Instrum. **55**, 952 (1984).

[7] O.V. Lounasmaa: "Experimental Principles and Methods Below 1K", Chap. 7. (Academic Press, 1974).

[8] R. De Bruyn Ouboter, A. Th. A.M. De Waele in: "Progress in Low Temperature Physics". Vol.VI pp.243-288.

[9] J. Clarke in: "Superconductor Applications: SQUIDs and Machines", B.B. Schwartz and S. Foner ed., (New York: Plenum, 1977), pp.67-124.

[10] J. Bardeen, L.N. Cooper and J.R. Schrieffer, Phys. Rev. **108**, 1175 (1957).

[11] I. Giaever, Phys. Rev. Lett. **5**, 147, 464 (1960).

[12] W.C. Steward, Appl. Phys. Lett. **12**, 277 (1968);
D.E. Mc Cumber, J. Appl. Phys. **39**, 3113 (1968).

[13] J.E. Zimmermann, P. Thiene and J.T. Harding, J. Appl. Phys. **41**, 1572 (1970).

[14] R.P. Giffard, R.A. Webb and J.C. Weatley, J. Low Temp. Phys. **6**, 553 (1972).

[15] D. Duret, P. Bernard and D. Zenatti, Rev. Sci. Instr. **46**, 417 (1980).

[16] J. Kurkijärvi and W.W. Webb, Proc. Appl. Supercond. Conf. IEEE,1972, p.581.

[17] L.D. Jackel and R.A. Buhrman, J. Low Temp. Phys. **19**, 201 (1975).

[18] T.D. Clark and L.D. Jackel, Rev. Sci. Instr. **46**, 1249 (1975).

[19] SHE Corp. (BTI), San Diego, USA.

[20] Cryogenic Consultants Ltd., London, U.K.

[21] L.E.T.I., Grenoble, France

[22] Quantum Design, San Diego, USA.

[23] C.D. Tesche and J. Clarke, J. Low Temp. Phys. **29**, 301 (1977).

[24] J. Clarke, W.M. Goubeau and M.B. Ketchen, J. Low Temp. Phys. **25**, 99 (1976).

[25] K.K. Likharev and V.K. Semenov, JETP Lett. **15**, 442 (1972).

[26] J. Clarke, Physica **126B**, 441 (1984).

[27] J.E. Zimmermann and A.H. Silver, Phys. Rev. **141**, 367 (1966).

[28] J. Clarke, ı ..... Mag. **13**, 115 (1966).

[29] S.K. Dekker and J.E. Mercereau, Appl. Phys. Lett. **25**, 527 (1974).

[30] W. Richter and G. Albrecht, Cryogenics **15**, 148 (1975).

[31] M.B. Ketchen, T. Kopley and H. Ling, Appl. Phys. Lett. **44**, 1008 (1984).

[32] J. Clarke and G. Hawkins, Phys. Rev. **B14**, 2826 (1976).

[33] M. Taber and B. Cabrera, Rev. Sci. Instr. **56**, 1835 (1985).

[34] For a review, see J. Clarke, IEEE Trans. Magn. **MAG19**, 288 (1983).

[35] For a review, see S.J. Williamson, L. Kaufman, J. Magn. Magn. Mater. **22**, 129 (1981); J. Clarke, Physics Today March 1986, p.36.

[36] For a review, see "Magnetic Monopoles" R.A. Carrigan and W.P. Trower ed. (Plenum, N.Y., 1983).

[37] B. Cabrera, Phys. Rev. Lett. **48**, 1378 (1982).

[38] O. Avenel and E. Varoquaux, ICEC11, Berlin, Klipping G., Klipping I. eds. (Butterworth, 1986), P.587.

[39] R. Kubo, J. Phys. Soc. Japan **12**, 570 (1957).

[40] M. Ocio, H. Bouchiat and P. Monod, J. Phys. Lett. (France) **46**, 647 (1985).

[41] W. Reim, R.H. Koch, A.P. Malozemoff, M.B. Ketchen and H. Maletta, Phys. Rev. Lett. **57**, 905 (1986).

[42] Ph. Réfrégier and M. Ocio, Revue Phys. Appl. **22**, 367 (1987).

[43] L. Landau and E. Lifshitz in "Electrodynamics of Continuous Media, Ch.VII (Pergamon Press, 1960).

[44] M. Ocio and J. Hammann, Rev. Sci. Instr. **56**, 1367 (1985).

[45] A. Davidson, R.S. Newbower and M.R. Beasley, Rev. Sci. Instr. **45**, 838 (1974).

TABLE CAPTION

Table I Principal characteristics of selected r.f. and d.c. SQUIDs, whose energy resolution is displayed in Fig.11.

TABLE I

SQUID	L_i μH	M_i nH	k	ε $J\ Hz^{-1}$	$S_\phi^{1/2}$ $\Phi_0 Hz^{-1/2}$	Slew rate $\Phi_0 s^{-1}$
r.f. SHE 19 MHz	2	20	0.65	10^{-28}	10^{-4}	$3\ 10^5$
r.f. C.C. Ltd. 20 MHz	1.5	15	0.6	10^{-28}	10^{-4}	$3\ 10^5$
r.f. LETI 100 – 200 MHz	1	10	0.65	$2\ 10^{-28}$	$1.5\ 10^{-4}$	$> 10^{-4}$
r.f. SHE + QD electronics 210 MHz	2	20	0.65	$2\ 10^{-29}$	$4\ 10^{-5}$	$5\ 10^5$
d.c. SHE	2	20	0.65	10^{-30}	$1.5\ 10^{-5}$	$3\ 10^5$
d.c. (F. Wellstood et al [6])	0.12	6		10^{-31}	$4\ 10^{-6}$	$3\ 10^6$
d.c. (M.B. Ketchen et al [5])	0.19	3.8	0.93	$1.6\ 10^{-32}$	$8\ 10^{-7}$	

FIGURE CAPTIONS

Fig.1 : I-V characteristics of Josephson junctions: a) tunnel junction; b) shunted tunnel junction or weak link.

Fig.2 : Examples of Josephson junctions: a) shunted tunnel junction; b) Dayem microbridge; c) point contact junction.

Fig.3 : a) Configuration of r.f. SQUID; b) total flux ϕ versus applied flux ϕ_{ext} for $LI_c/\phi_0 \sim 0.8$. The arrows shows the variations of ϕ when ϕ_{ext} is first increased and then decreased.

Fig.4 : a) r.f. coupling of the r.f. SQUID; b) tank voltage amplitude as a function of ϕ_{dc} for two optimal amplitudes of i_{rf}.

Fig.5 : a) Q-meter coupling of the r.f. SQUID; b) SWR-meter coupling of the r.f. SQUID; the intermediate line coil L_L is used to transform the tank circuit impedance to 50 Ω.

Fig.6 : Schematic of the r.f. SQUID electronics in a flux-locked loop; b) Principle of the flux modulation technique.

Fig.7 : a) Configuration of a d.c. SQUID; b) equivalent circuit.

Fig.8 : Behavior of a d.c. SQUID when the self inductance L can be neglected.

Fig.9 : Behavior of a d.c. SQUID in the general case, for $\beta = LI_c/\phi_0 = 1$.

Fig.10 : Schematics of d.c. SQUID coupling: a) tuned tank circuit; b) wide band transformation.

Fig.11 : Energy resolution of selected r.f. and d.c. SQUIDs; 1) r.f. SHE; 2) r.f. Cryogenic consultants Ltd.; 3) r.f. LETI; 4) r.f. SHE with Quantum Design electronics; 5) d.c. SHE; b) Planar d.c. Ref.[6]; 7) Planar d.c. Ref.[5].

Fig.12 : a) Flux transformer; b) cylindrical and c) planar first order gradiometers; recurent generation of d) cylindrical and e) planar gradiometers.

Fig.13 : Measurement of static magnetization.

Fig.14 : a) Measurement of noise; b) equivalent circuit.

Fig.15 : a) Principle of the mutual inductance bridge; b) Schematics of a practical realization (Ref.[14]).

Fig.16 : a) Principle of an automatic feedback simplified mutual inductance bridge; b) schematics of the two channels electronics (Ref.[44]).

Fig.17 : a) Principle of the impedance bridge; b) Schematics of a practical realization (Ref.[14]).

Fig.18 : Principle of the SQUID voltmeter.

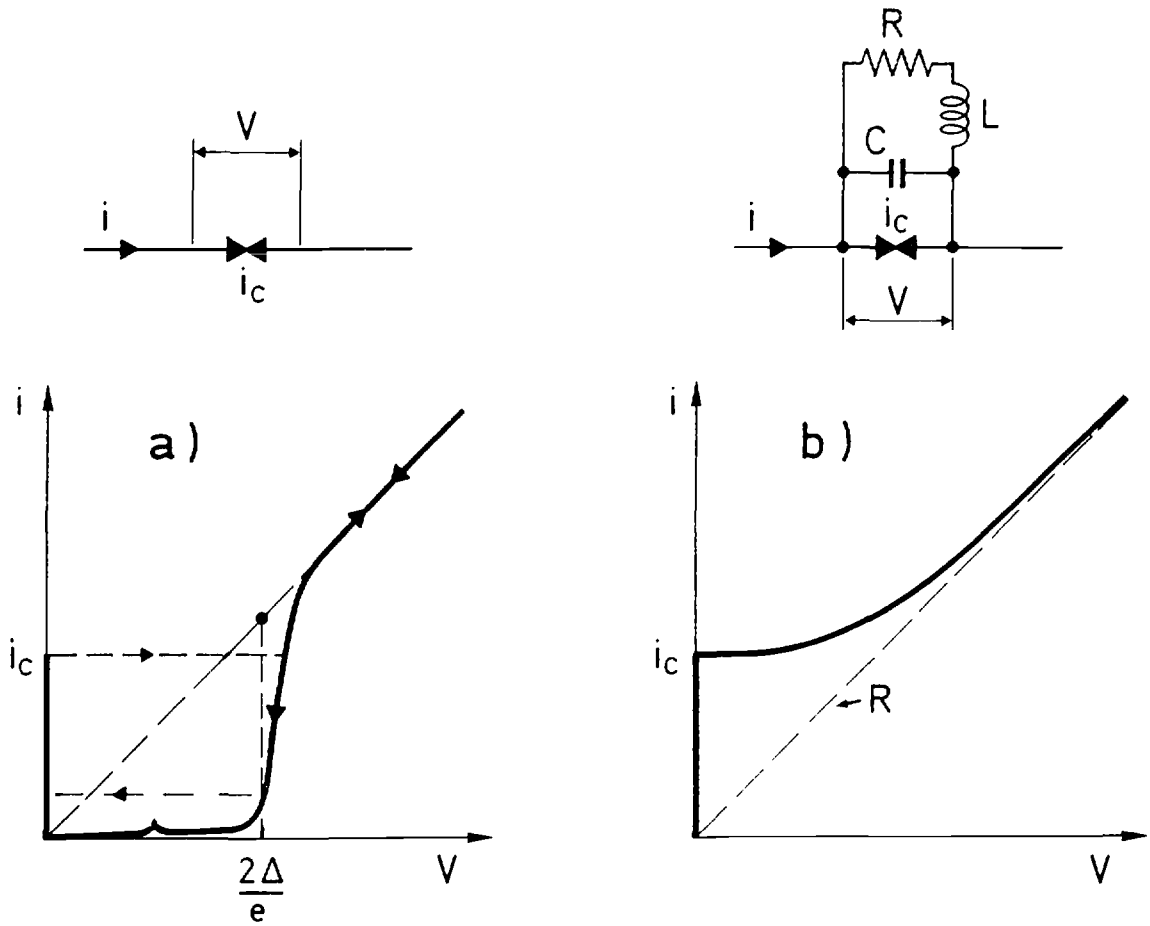

Figure 1

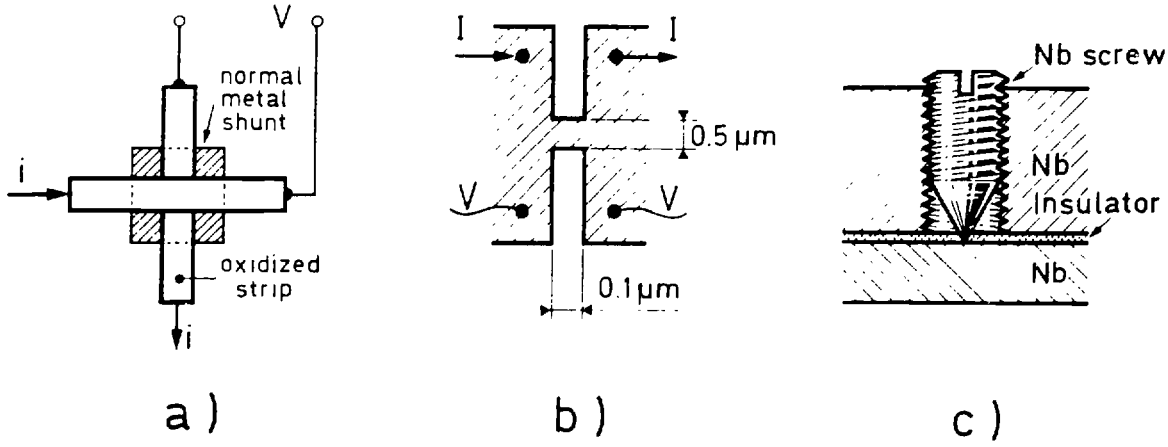
V
normal
metal
shunt
i
oxidized
strip
i
a)
I
I
0.5 µm
V
V
0.1µm
b)
Nb screw
Nb
Insulator
Nb
c)

Figure 2

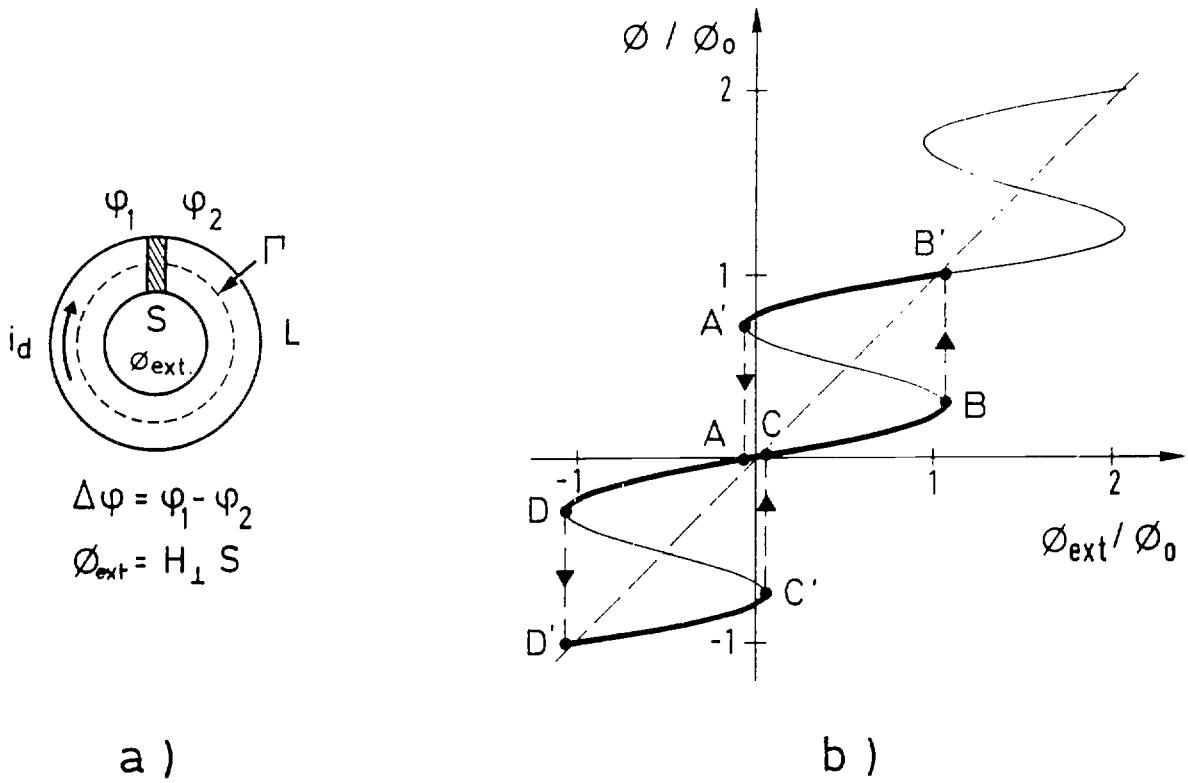

Figure 3

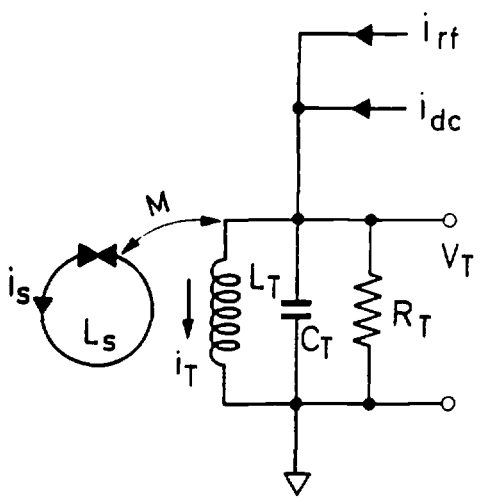

a)

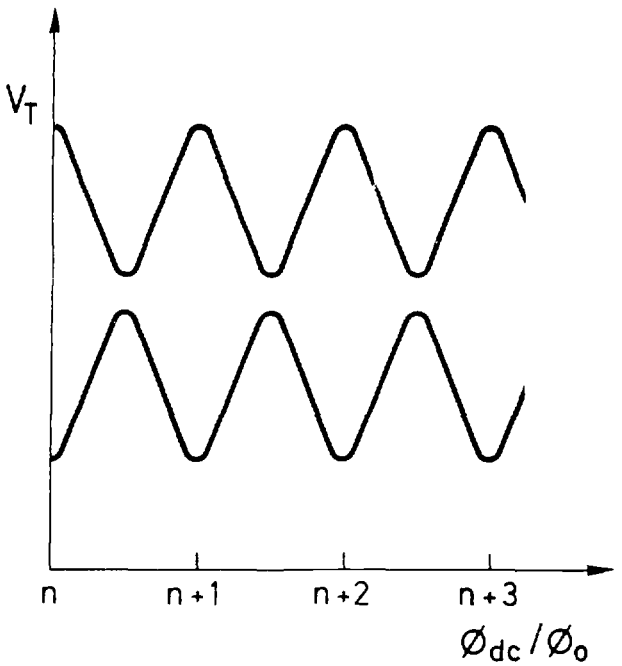

b)

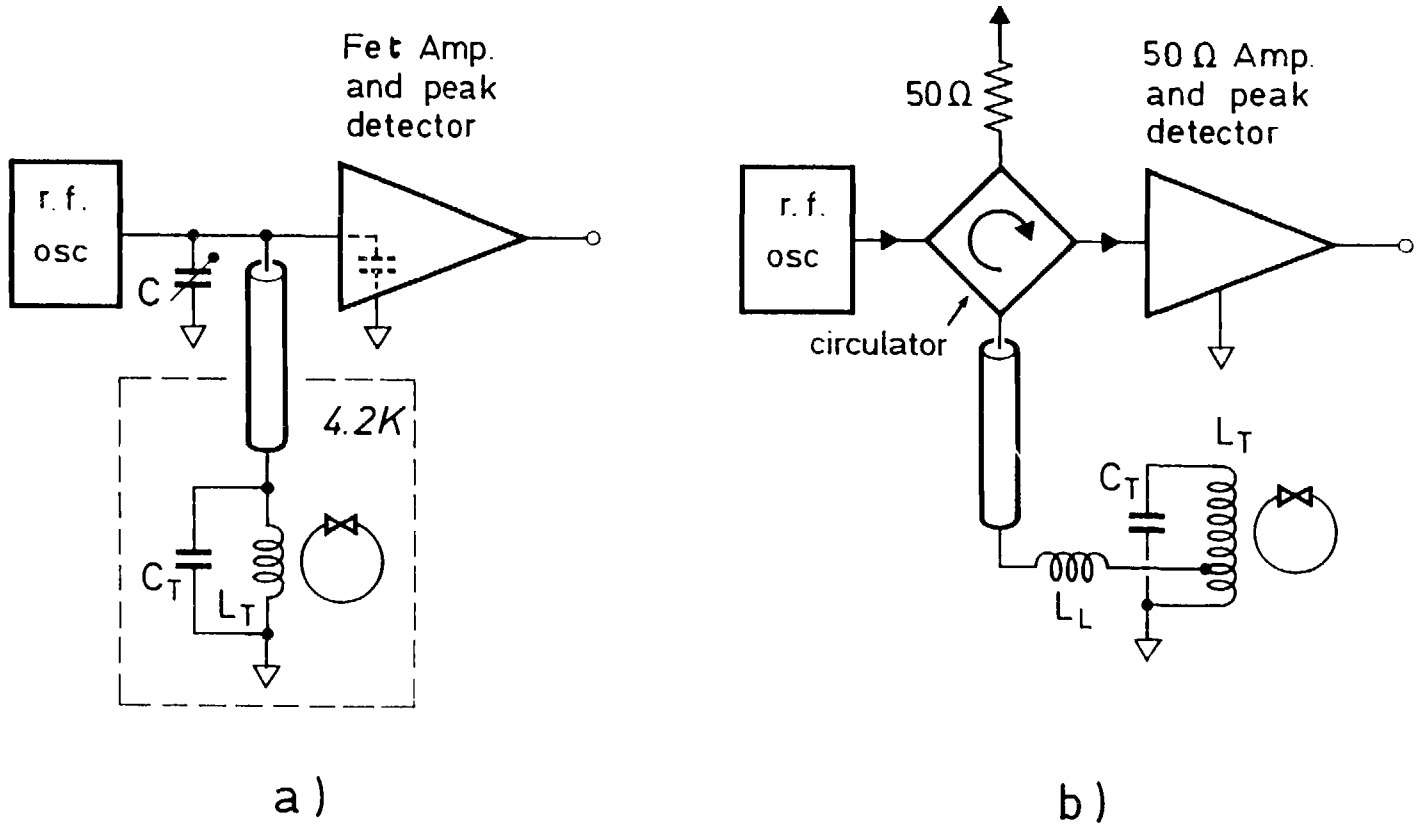
Fet Amp.
and peak
detector
r.f.
osc
C
4.2K
C_T
L_T
a)
50Ω
50Ω Amp.
and peak
detector
r.f.
osc
circulator
L_T
C_T
L_L
b)

Figure 5

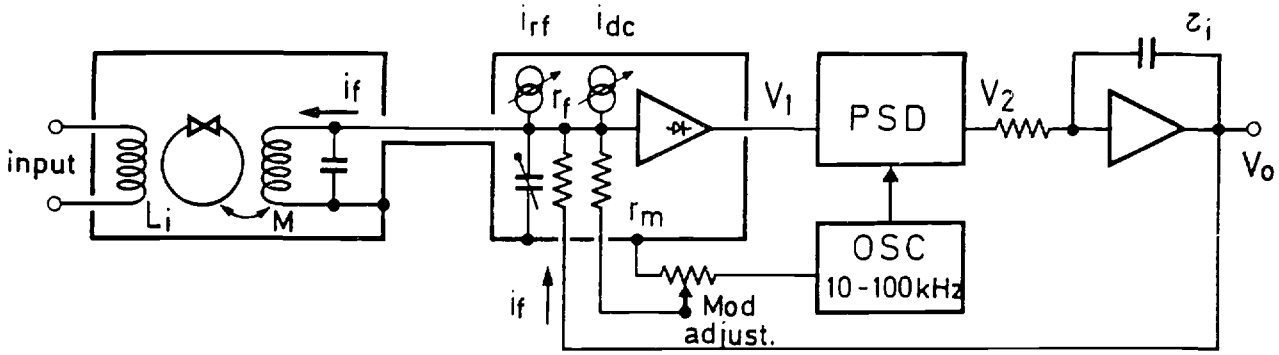
input
Li
M
if
irf
idc
rf
rm
V1
PSD
V2
zi
Vo
OSC
10-100kHz
Mod
adjust.
if

a)

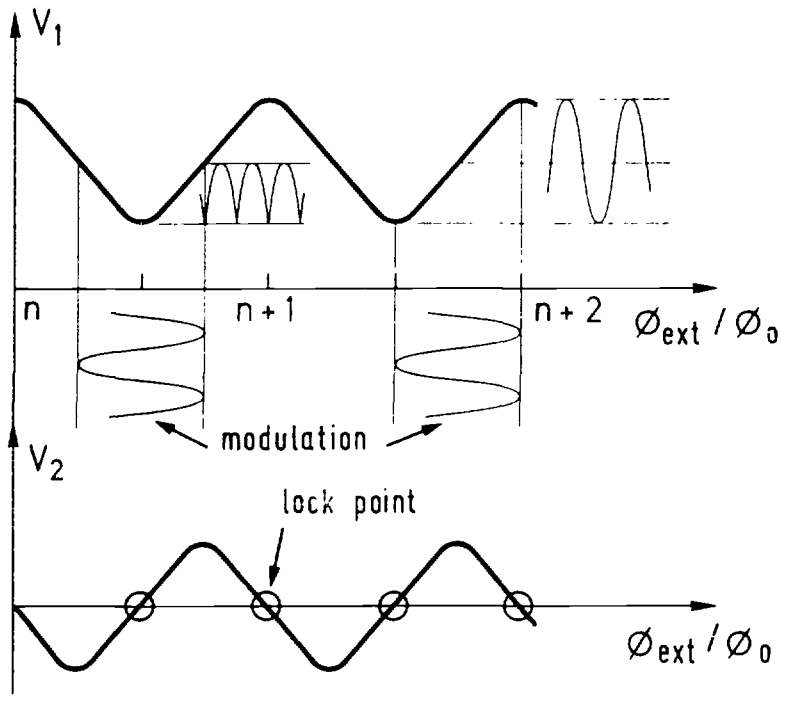
V1
n
n+1
n+2
Øext / Ø0
modulation
V2
lock point
Øext / Ø0

b)

Figure 6

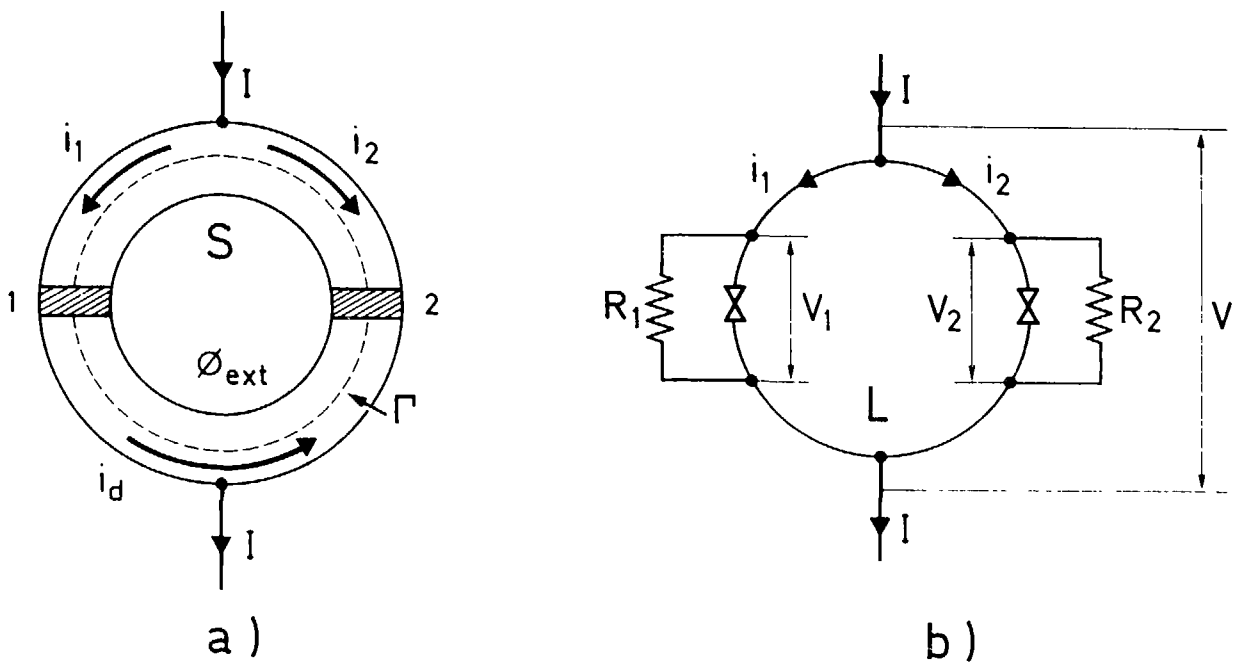

Figure 7

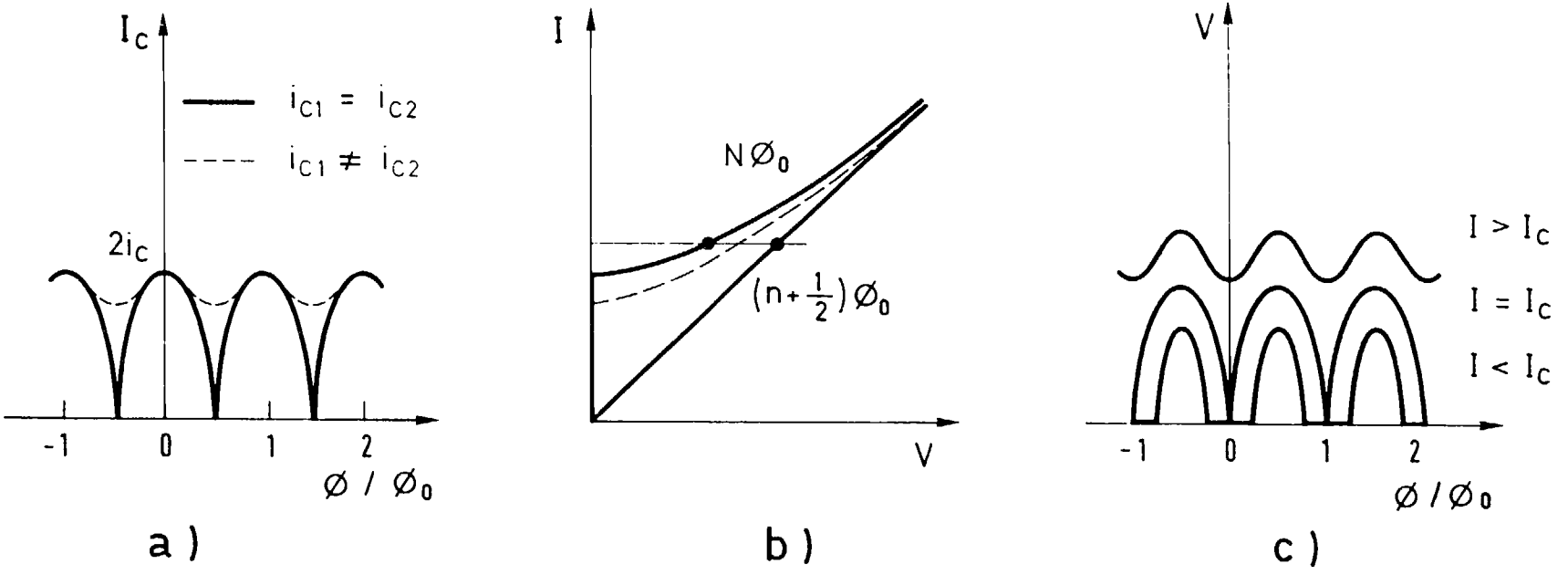
I_c
$i_{c1} = i_{c2}$
$i_{c1} \neq i_{c2}$
$2i_c$
-1
0
1
2
Φ / Φ_0
a)
I
$N\Phi_0$
$(n+\frac{1}{2})\Phi_0$
V
b)
V
$I > I_c$
$I = I_c$
$I < I_c$
-1
0
1
2
Φ / Φ_0
c)

Figure 8

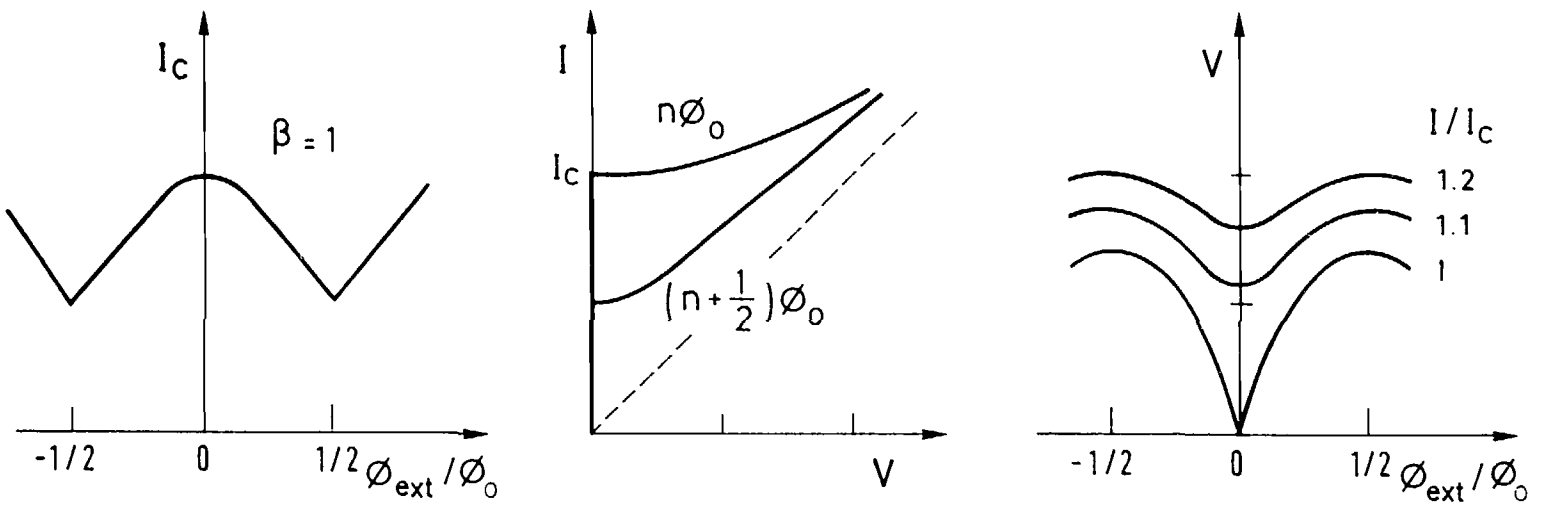
I_c
$\beta = 1$
-1/2
0
1/2 Φ_{ext}/Φ_o
I
I_c
$n\Phi_o$
$(n+\frac{1}{2})\Phi_o$
V
V
I/I_c
1.2
1.1
1
-1/2
0
1/2 Φ_{ext}/Φ_o

Figure 9

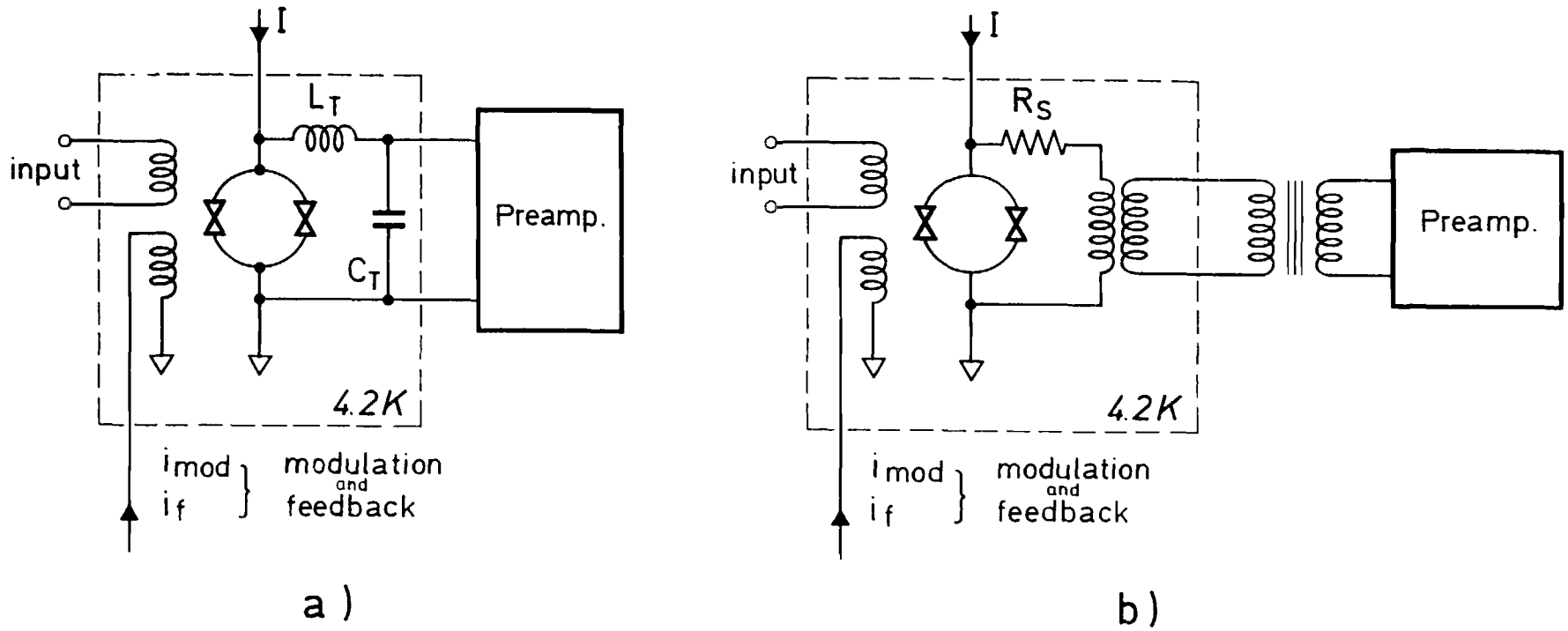
I
L_T
input
Preamp.
C_T
4.2K
i_{mod}
i_f
modulation
and
feedback
a)
I
R_S
input
Preamp.
4.2K
i_{mod}
i_f
modulation
and
feedback
b)

Figure 10

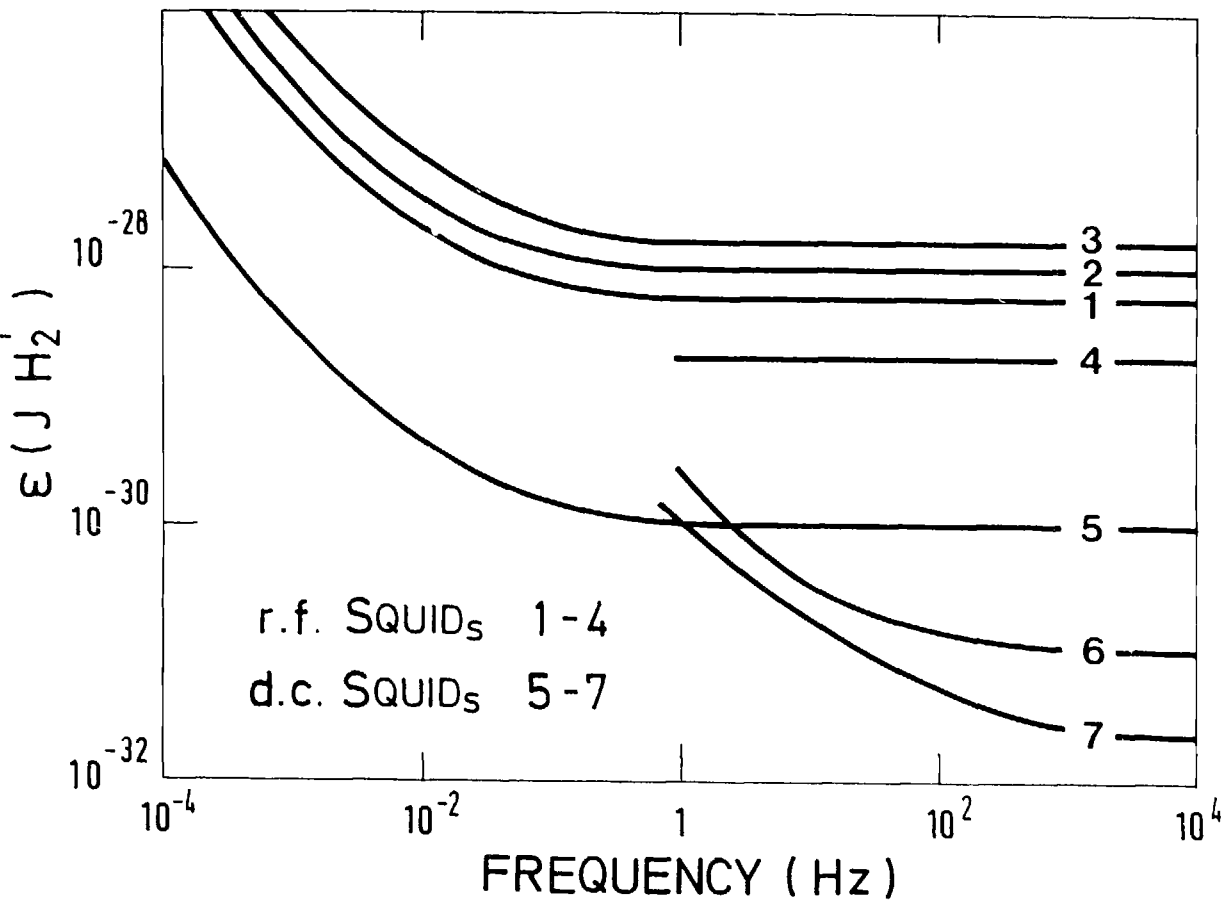
ε (J H$_2^{-1}$)
10^{-28}
10^{-30}
10^{-32}
r.f. SQUIDs 1-4
d.c. SQUIDs 5-7
3
2
1
4
5
6
7
10^{-4}
10^{-2}
1
10^{2}
10^{4}
FREQUENCY (Hz)

Figure 11

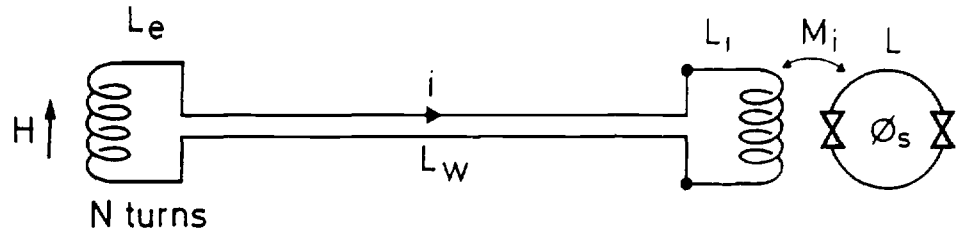

a)

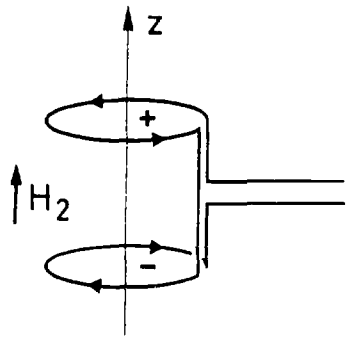

b)

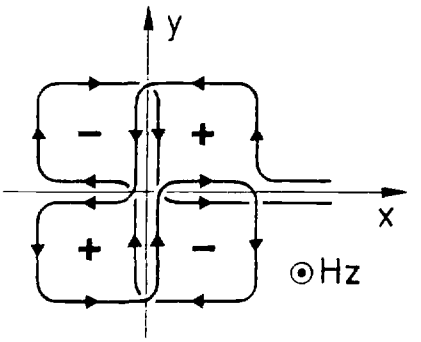

c)

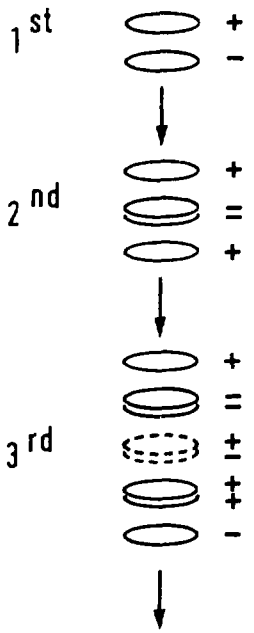

d)

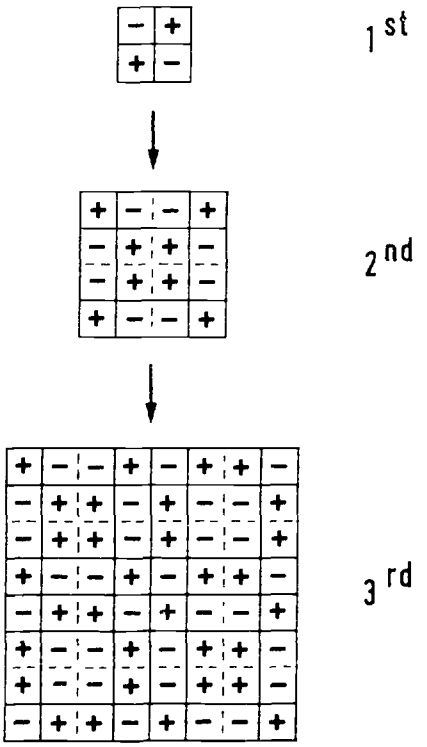

e)

Figure 12

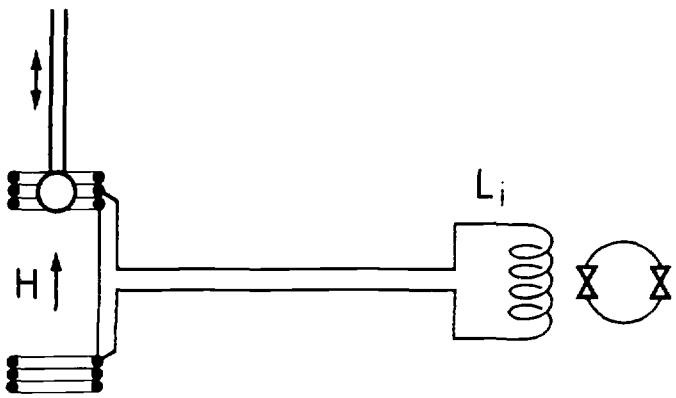

Figure 13

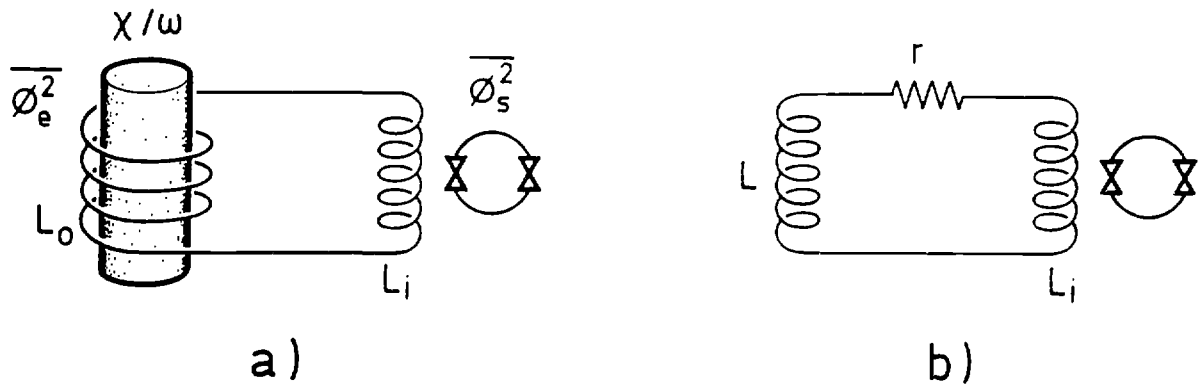

Figure 14

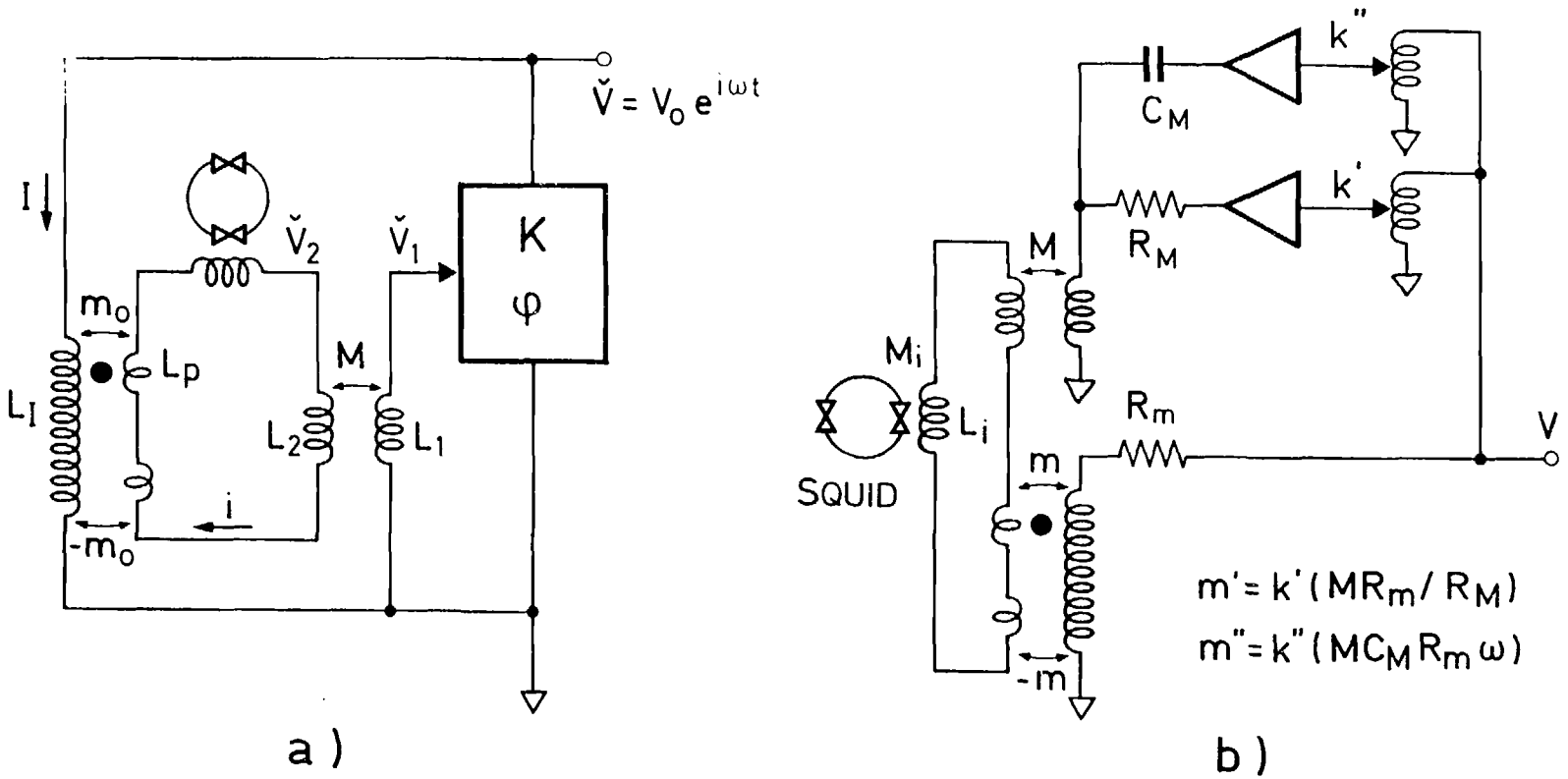
V̌ = V₀ e^{iωt}
I
V̌₂
V̌₁
K
φ
m₀
Lp
M
L₁
L₂
L_I
i
-m₀
a)
k''
C_M
k'
R_M
M
M_i
L_i
R_m
V
SQUID
m
-m
m' = k' (MR_m / R_M)
m'' = k'' (MC_M R_m ω)
b)

Figure 15

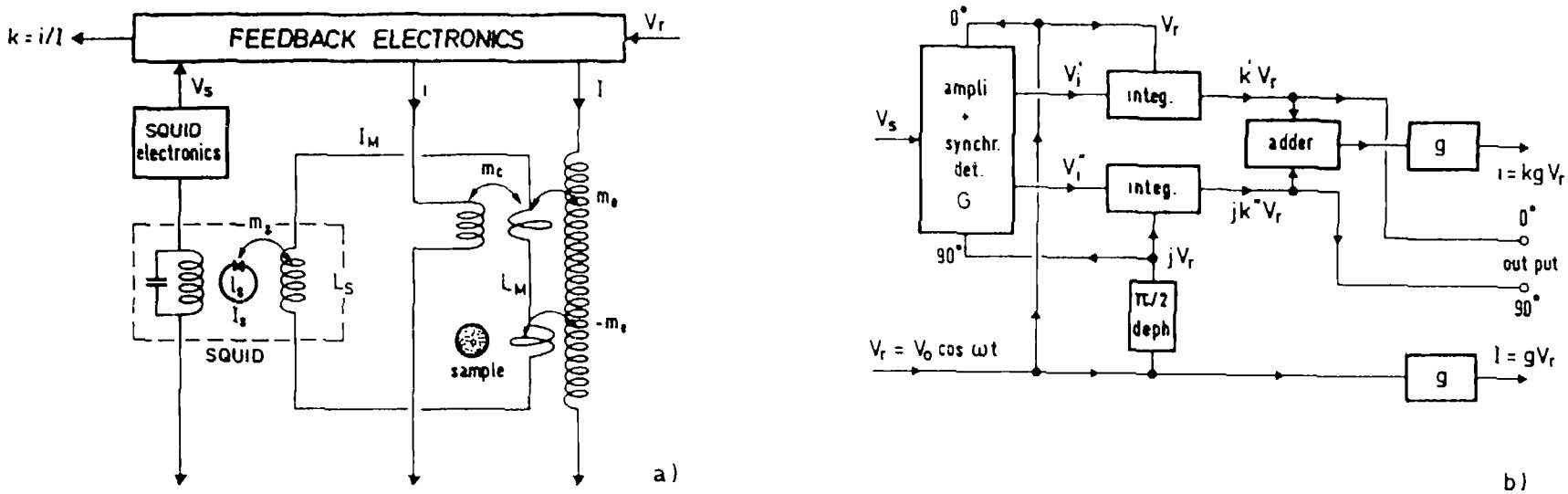
k = i/I
FEEDBACK ELECTRONICS
Vr
Vs
SQUID electronics
I
I
IM
mc
me
ms
Ls
LM
-me
SQUID
sample
a)
0°
Vr
ampli + synchr. det. G
Vs
V'i
integ.
k' Vr
adder
g
I = kg Vr
V"i
integ.
jk" Vr
0°
out put
90°
90°
jVr
π/2 deph
Vr = Vo cos ωt
I = gVr
g
b)

Figure 16

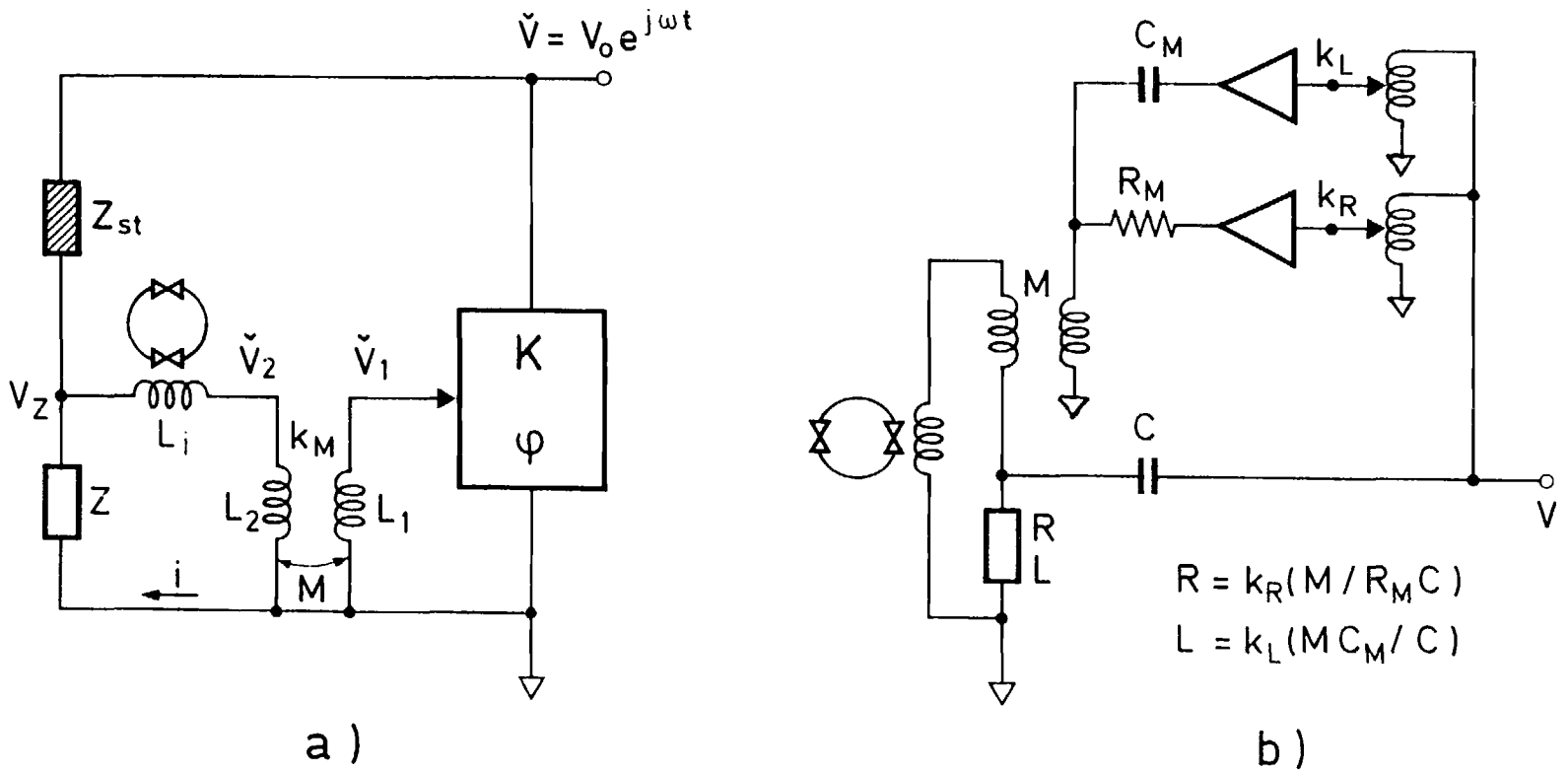
V̌ = V₀ e^{jωt}
Z_st
V̌₂
V̌₁
K
φ
V_Z
L_i
k_M
Z
L₂
L₁
i
M
a)
C_M
k_L
R_M
k_R
M
C
V
R
L
R = k_R(M / R_M C)
L = k_L(M C_M / C)
b)

Figure 17

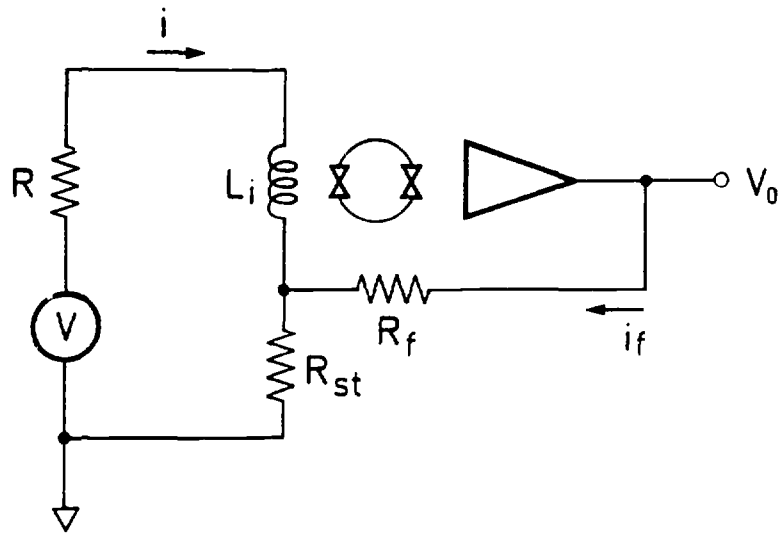

Figure 18